Microstructure and Mechanical Properties of Heat Treated FSLA Steel Produced by the Binder Jet Process

Chris Schade[1] Chris.Schade@hoeganaes.com; Kerri Horvay[1] Kerri.Horvay@hoeganaes.com; Tom.Murphy[1] Tom.Murphy@hoeganaes.com; Corina Junghetu[2] Corina.Junghetu@hoeganaes.com

[1] (Hoeganaes Corporation, USA)
[2] (Hoeganaes Corporation Europe, Romania)

Abstract

An alloy, called FSLA (free-sintering low-alloy), was designed and implemented for use with binder jet printing. This work focuses on various heat treatments that can be utilized with the alloy to produce a range of properties for various applications. The microstructure of the alloy can be varied post-sintering, by heat treatment, to give a wide range of mechanical properties that are suitable for automotive components. Balancing the carbides in the structure along with the amounts of ferrite and martensite/bainite give a range of ultimate tensile strengths from approximately 490 to 1000 MPa. Unlike other low alloy steels, the material has been designed to have a high degree of sinterability which allows densities of the order of 98% to be reached while sintering at temperatures typically used in metal injection molding (1380 °C).

Introduction

Metal Binder Jetting (MBJ) has garnered more interest as an additive manufacturing technique primarily due to the increased speed at which material can be printed and the wider range of materials that can be processed when compared to techniques like Laser Powder Bed Fusion (LPBF). However, because of the low as-printed density, the sintering process generally requires longer times and higher temperatures than conventional processes like metal injection molding (MIM). In addition, the binders utilized by the commercially available MBJ printers often interact with the powder surface, complicating the sintering process and requiring additional development efforts on the part of the end user. Physical attributes of the powder such as apparent density, tap density and flowability of the powder impact how the material interacts with the recoater in the printer. For the most part this has limited the availability of materials for MBJ to those which are developed with the printer itself such as 316L stainless steel. As mentioned previously the increase in printing speed of MBJ, makes the process attractive for serial production of cost-sensitive parts, such as those used by the automotive industry. Due to the decoupling of shaping and solidification into a two-step process (printing/sintering), production throughput can be increased 10-50 times compared with other AM technologies e.g., LPBF. In addition, BJT is not limited to alloys that are weldable but can utilize a wider range of materials. To achieve high densities (>98% relative density) fine powders are used with a mean particle size, d_{50}, ranging from 10-15 μm. Utilizing fine powders results in a superior surface quality, about 20% better than LPBF.

Because of these benefits, the automotive industry is now more actively engaged in evaluating BJT for production of automotive parts. In particular, because of the ability of 3D printing to produce designs that are conducive to weight reductions, a particular interest of the automotive makers is the application of sheet material for body and chassis parts. The steels used for these applications are generally classified as Advanced High Strength Steels (AHSS).
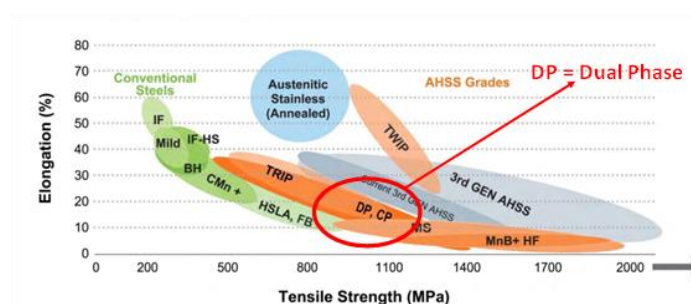

Figure 1: Steel Strength Ductility Diagram, illustrating the range of properties available from today's AHSS grades [1].

Advanced high-strength steels (AHSS) or micro-alloyed steels, generally give superior mechanical properties utilizing low levels of alloy content coupled with thermo-mechanical processing (typically rolling in combination with accelerated cooling). Dual-phase (DP) steels are considered a subclass of AHSS and exhibit a microstructure consisting of a hard phase (primarily martensite and/or bainite) in a matrix of ferrite (Figure 1) [2-4]. Due to their composite microstructures, dual-phase steels exhibit excellent mechanical properties with ultimate tensile strengths (UTS) generally dependent primarily on the volume fraction of martensite/bainite. These steels are therefore classified according to their ultimate tensile strength; for example, DP500 has a UTS of approximately 500 MPa while DP1000 would have an approximate UTS of 1000 MPa.

In previous papers an alloy called FSLA (Free Sintering Low Alloy) was introduced for MBJ which was comparable in properties to DP600 (i.e., UTS = 600 MPa) [5]. Unlike other low alloys steels, the chemistry of the FSLA alloy was tailored to have a mixed microstructure of approximately 50 volume percent ferrite and 50 volume percent austenite at the sintering temperatures. Work by previous authors had suggested that the increase in grain boundary area between the austenite and ferrite would increase the diffusion and lead to higher sintered densities. This was proven to be the case as the MBJ- FSLA had superior sintered density than other low alloy steels [6-7]. The ferrite stabilizing elements (chromium, molybdenum, and silicon) were all chosen because of their hardenability characteristics which allowed for the transformation of the austenite to martensite at moderate cooling rates. The alloy chemical composition allowed for intercritically annealing in a two-phase region of austenite and ferrite. With appropriate cooling rate, the austenite will transform to martensite (and/or bainite) and a final microstructure of different levels of ferrite and martensite/bainite (the typical microstructure of dual phase steels) can be accomplished. For the previous work target values for DP600 were obtained by intercritically annealing at 850 °C and cooling at a rate of 1.3 °C/sec. The properties and microstructure of the material processed in this way are shown in Table I and Figure 2 respectively.

Table I: Mechanical properties of FSLA compared to Wrought DP600 (produced by Salzgitter [8])

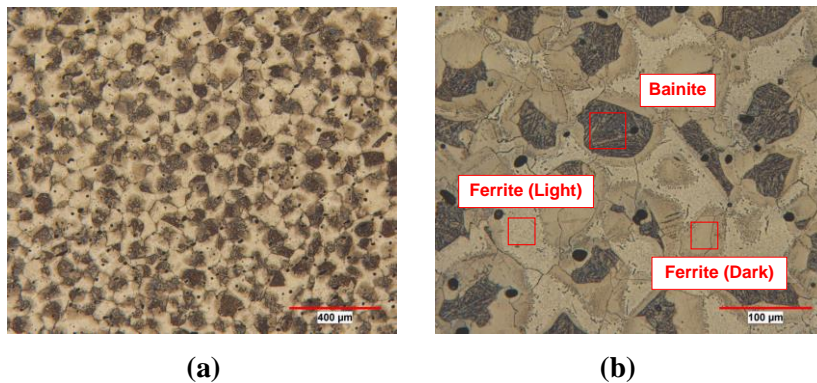|	UTS [MPa]	0.2%YS [MPa]	Elongation [%]	Hardness [HRA]
Wrought DP600 (Salzgitter)[8]	580-670	330-470	24 (min)	---
FSLA MBJ (6 runs)	687 ± (8.3)	395 ± (8.7)	19.7 ± (0.4)	51 ± (1)

(a)   (b)

Figure 2: Mechanical Properties and Microstructure of FSLA alloy intercritically annealed at 850 °C and cooled at a rate of 1.3 °C/s. (a) general microstructure and (b) higher magnification identifying the bainite as well as the two types of ferrite dislocated (dark) and non-dislocated.

The target properties of the DP600 were met by this development work, but the ability to heat treat the FSLA alloy in the two-phase region lends itself to further investigation into the achievable properties of this alloy. As mentioned in the introduction, an alloy processed to achieve a range of mechanical post-printing is desirable to save on printer development work. Therefore, this paper details additional heat treatment routines that can expand the range of ultimate tensile strength and ductility of the FSLA alloy without changes to its composition or printing parameters.

2. Experimental Details

Powders utilized in this study were air melted and gas atomized with nitrogen. Chemical analysis and powder properties are listed in Table II.

Table II: Powder properties of Air Melted- Gas (nitrogen) Atomized FSLA.

Material	Apparent Density g/cm³	Tap Density g/cm³	Carbon wt.%	Sulfur wt.%	Oxygen wt.%	Nitrogen wt.%	d_{10} Micrometers	d_{50} Micrometers	d_{90} Micrometers
FSLA Powder	3.2	4.9	0.14	0.007	0.06	0.01	5.7	14.0	24.4

Material	Mn	Cr	Ni	Mo	Nb	V	Si
FSLA Powder	0.20	1.60	0.06	1.45	0.18	0.18	1.64

All test samples were printed on an HP Multi Jet Fusion Printer, with a water-based binder at a 50-micrometer layer thickness.

Test pieces were sintered at DSH Technologies utilizing MIM3045T furnaces from Elnik Systems. These furnaces combine the thermal debind and the sinter process in one furnace. The equipment has a maximum temperature of 1600 °C with partial pressure or vacuum control. The furnace is an all-metal process zone with atmosphere capabilities of pure hydrogen, nitrogen, argon, or vacuum environments. For this study the test pieces were sintered in a high temperature Elnik MIM at 1380 °C for 30 minutes in an atmosphere of 95 vol.% nitrogen / 5 vol.% hydrogen.

For continuous heat treatment, a high temperature Abbott continuous-belt furnace was used at indicated temperatures for 30 minutes in an atmosphere of 95 vol.% nitrogen / 5 vol.% hydrogen.

Prior to mechanical testing, green and sintered densities, dimensional change (DC), and apparent hardness were determined on the tensile and transverse rupture (TR) samples. Five tensile specimens (flat dogbones/unmachined) and five TR specimens were evaluated for each composition. The densities of the green and sintered steels were determined in accordance with MPIF Standard 42. Tensile testing followed MPIF Standard 10, and apparent hardness measurements were made on the tensile and TR specimens, in accordance with MPIF Standard 43.

Porosity measurements were made on metallographically prepared cross-sections removed from entire test parts. A Clemex automated image analysis system was used to measure and map the porosity on as-prepared surfaces using a predetermined grey level to separate the dark void space from the highly light reflective metallic regions. This provided the opportunity to estimate the pore content in both the sample volume and in localized regions.

Specimens for microstructural characterization were prepared using standard metallographic procedures. Subsequently, they were examined by optical microscopy in the polished and etched (2 vol.% nital / 4 wt.% picral) conditions.

In addition, the microstructure was revealed, and color was used to separate the transformation products with a two-step, etch/stain, process. First, the microstructure was defined with a light pre-etch by immersing the sample in Vilella's Reagent (5 mL HCl + 1 g picric acid + 100 mL ethyl alcohol), rinsing with warm water, and drying with filtered compressed air. In the second step, the pre-etched sample was immersed in a freshly prepared solution of 10 g sodium metabisulphite ($Na_2S_2O_5$) in 100 mL deionized or distilled water, rinsed with warm water and alcohol, then dried with filtered compressed air.

3. Sintering Process and Heat Treatment

One of the unique features of the FSLA alloy is the wide range of temperatures in which the alloy can be heat treated in a two-phase region of austenite and ferrite. This is shown by the Calphad diagram in Figure 3. When heat treated at a temperature of approximately 870 °C, the microstructure of the FSLA alloy is > 90% ferrite. Conversely, when held at temperatures near 1150 °C the microstructure is ~ 90% austenite which can transform to either bainite or martensite depending on the cooling rate. One of the key features of dual phase steels is the ability to vary the mechanical properties by changing the levels of martensite and ferrite. If a material of higher strength and hardness is required intercritical annealing is performed at a temperature at which there is a high level of austenite that can transform during cooling. If a material with lower strength but better ductility is required, an intercritical anneal temperature which favors the formation of the softer ferrite phase is chosen. In order to evaluate the range of properties the FSLA alloy could exhibit it was decided to test the extreme

differences in the phases; an alloy that was ~ 90% ferrite and an alloy that was 90% transformation products (martensite/bainite).
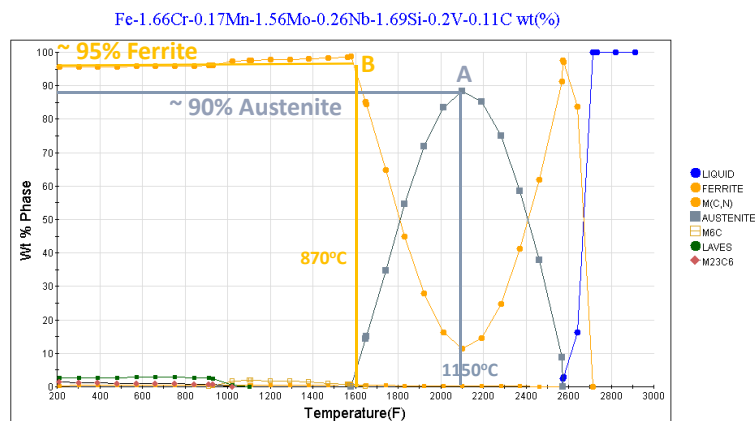

Figure 3: CALPHAD generated diagram for the phases present at various temperatures for the FSLA alloy chemical composition shown in Table II.

The first set of experiments involved heating the FSLA alloys to a temperature of around 1200 °C which corresponds to point "A" on Figure 3. At this temperature, at equilibrium, the FSLA microstructure should consist of approximately 85% austenite, which can then transform to martensite/bainite depending on the cooling rate. It is important to note that the chromium, molybdenum and silicon levels in the alloy combine to give a high hardenability as this alloy can transform with only furnace cooling (no quenching). This is a distinct advantage of this alloy formulation as these alloy elements also allow for the proper phase balance at the sintering temperature to enhance diffusion by formation of austenite/ferrite phase boundaries.

However, the diagram in Figure 3 is an equilibrium diagram and does not account for the kinetics of the phase transformations to take place. The initial microstructure of the test specimens that exists after sintering and subsequent cooling from the sintering temperature is a mixture of transformation products (martensite/bainite) and ferrite. When the test specimens are heated to 1200 °C, both the transformation products and the ferrite need to change crystal structure to austenite. This is done by partitioning of elements and this takes time. To evaluate the amount of time needed to compete the transformations, sintered samples of the FSLA were heat treated for 1,2,3,4 and 5 hrs. at 1200 °C in a vacuum furnace, under a partial pressure of nitrogen. Tensile properties and hardness values were measured after each of the time increments. Quantitative metallography was used to determine the level of martensite in the specimens. Figure 4 shows the results of the experiments. Between 1-3 hours the martensite values fell far short of the predicted equilibrium values shown in Figure 3. After 3 hours the martensite volume fraction approached the 80% value predicted by the Calphad diagram. The ultimate tensile strength and hardness values reached a maximum at around 4-5 hours eventually achieving a UTS of 1050 MPa. It also should be noted that heat treating at various times leads to a variation on the amount of martensite which allows UTS strengths from 800 MPa in the as sintered condition to 1050 after 3-5 hours at 1200 °C. This flexibility in properties allows the same printed material to be used in a range of applications.

The mechanism for the different levels of formation of martensite is due to diffusion of the alloying elements most notably carbon, chromium, silicon and molybdenum. Carbon, which diffuses interstitially, has the biggest impact since it has both the greater mobility and also is the most effective element in hardening the martensite. The mechanism for the different levels of formation of martensite is due to diffusion of the alloying elements most notably carbon, chromium, silicon and molybdenum. Carbon, which diffuses interstitially, has the biggest impact since it has both the greater mobility and also is the most effective element in hardening the martensite.

Figure 5 shows a EPMA (Electron Probe Micro Analysis) results of a scan across both the ferrite and martensite grains for various times at 1200 °C. The graphs of the various elements show that carbon has the biggest variation between the ferrite and martensite grains reaching a maximum at 1 hr. with an amount almost double value of the ferrite (0.09% versus 0.045). In general, all elements seem to reach a value of equilibrium after three hours. Although the martensite should have its maximum
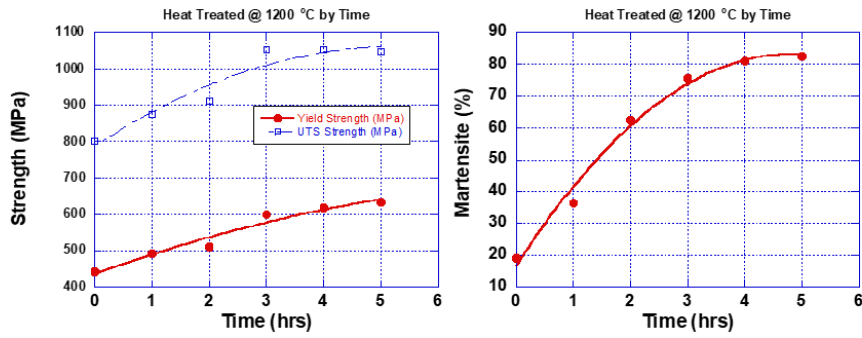
Figure 4: Effect of heat treatment time at 1200 °C on Tensile Strength (left) and amount of martensite (right).

hardness after 1 hr., the amount of martensite as shown increases and starts to level of after 3 hrs. Therefore, the maximum strength in the alloy is a combination of partitioning of the carbon to the austenite at high 1200 °C and the amount of martensite that is formed upon cooling.
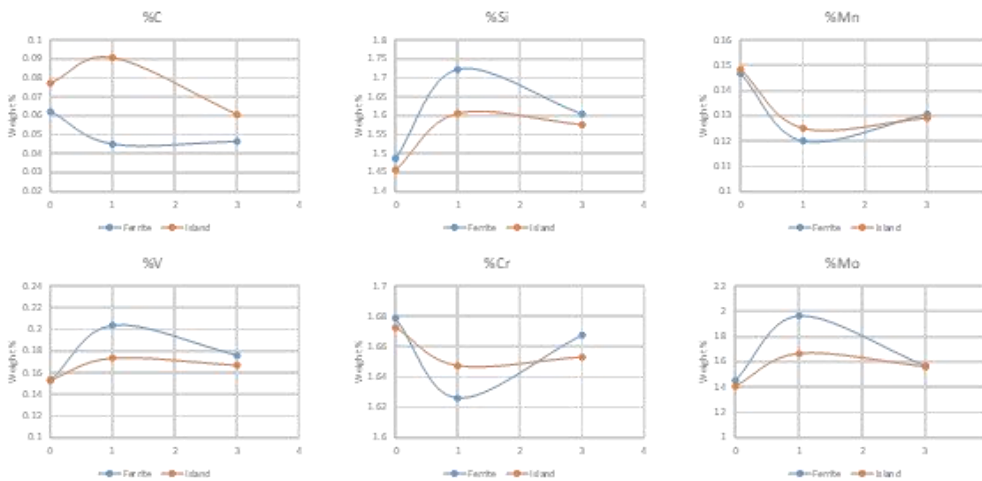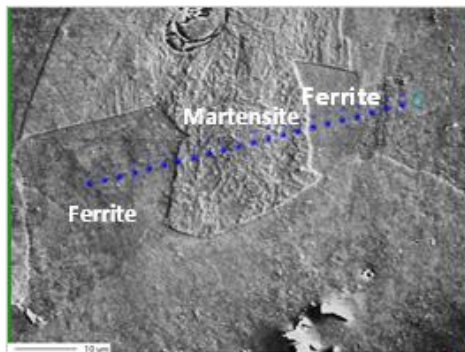

Figure 5: Scanning Electron Microscope image of ferrite and martensite phases with blue dots showing EPMA scans for chemistry (Top) and chemical analysis by EPMA (bottom) of various elements by hours heat treated (X-axis).

Since the diffusion of carbon can take place with both time and temperature, different levels of carbon in the martensite can be achieved by intercritically annealing for different times and temperatures, this increasing the variation in mechanical properties that can be achieved.

A second set of experiments were conducted in which the FSLA was intercritically annealed in a range of 800-900 °C. At this temperature the indication from Figure 3 (Point B) is that the microstructure of the alloy will be predominantly ferrite which will allow for a material with much higher level of ductility. This increase in ductility (elongation) is useful in the sheet metal components where the energy from impact needs to be absorbed (mainly the chassis area, such as bumpers). The microstructure of the FSLA alloy after the sintering process is a mixture of ferrite and some transformation products (usually bainite). Therefore, it was necessary to re-austenitize the samples, allowing the already transformed ferrite (from sintering) to transform to austenite and allowing for a maximum amount of ferrite to be

formed by holding at this temperature. For this reason, the samples were heated for 1 hour at 1200 °C followed by a furnace cool to an intercritical anneal temperature in a range of 800 to 900 °C. Holding at these temperatures allowed for the transformation of the high temperature austenite to ferrite. In order to maximize ductility, there is a necessity to balance the level of ferrite which predominates at the lower temperatures (800 °C) with the amount of carbide formation from elements like niobium, vanadium and molybdenum. The precipitates that form from these elements were useful in creating the high strength necessary in the DP980 type alloys, but hinder dislocation motion and therefore limit the ductility of the alloy at the range necessary to achieve the elongation values necessary for alloys such as DP480 (UTS = 480 MPa).

To optimize the mechanical properties, 3 intercritical anneal temperatures were used 825, 871 and 898 °C. The amount of ferrite was measured in specimens for all three temperatures as shown in Figure 6. At the lower temperatures (825 °C) the amount of ferrite was maximized at 92%. However, the number of carbides were increased. Conversely, at 898 °C, the carbides were minimized, but the level of ferrite was reduced to 71%. Since the ferrite dominates the ductility of the alloy it was decided to focus on intercritically annealing at the lower temperatures and trying to minimize the impact of the carbides on the strength.

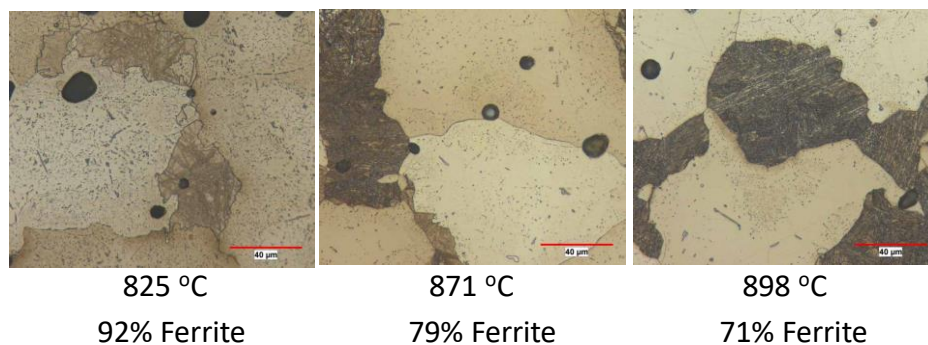| 825 °C | 871 °C | 898 °C |
| 92% Ferrite | 79% Ferrite | 71% Ferrite |

Figure 6: Effect intercritical anneal temperature on amount of ferrite phase and the level of carbides.

Having already established that the maximum amount of ferrite could be produced with intercritical anneal temperatures of around 800 °C, it was necessary to limit the impact of the carbides on increasing the tensile strength and reducing ductility. Based on thermodynamics, the formation of the carbides is inevitable, however limiting the size and frequency of the carbides was investigated in order to reach the target properties of a DP480 material. One obvious way to limit the carbide formation is to restrict the amount of carbon available to combine with the carbide forming elements such as chromium, silicon, molybdenum, vanadium and niobium. A method for reducing the carbon available is to make sure that the carbon content associated with the martensite is as high as possible. Therefore the variation of carbon in both the ferrite and the martensite was studied as a function of the time and temperature for the intercritical anneal. EPMA measurements were taken across the martensite grains at 800 °C for time intervals of 10 secs, 30, 60 and 120 mins. The sample isothermally held at 10 seconds was meant as a baseline measurement for the starting carbon. An example of a microprobe measurement is shown in Figure 7. Here the carbon can be seen to be lower in the ferrite and increases as the microprobe crosses the ferrite/martensite interface with a time of 2 hrs. (increase of 15%).
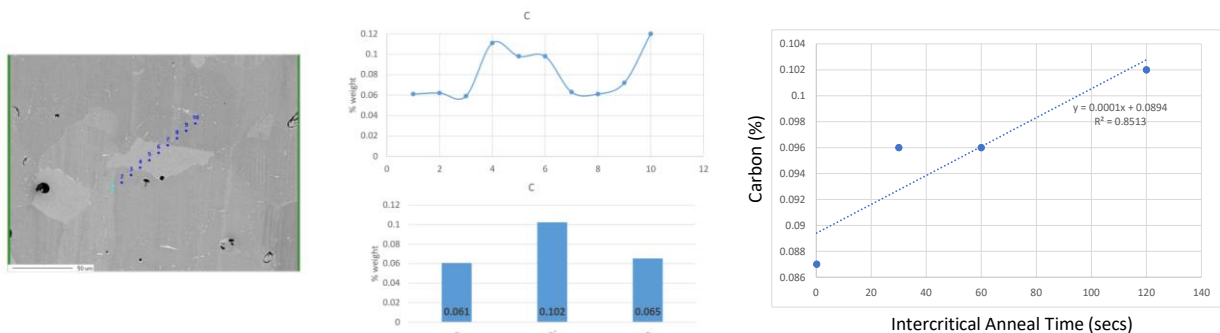

Figure 7: EPMA probe locations through ferrite and martensite grains (left) and accompanying carbon content (center). Carbon plot versus hold time at 800 °C (right).

maximum value achieved in the martensite grain. A plot of carbon content versus hold time at 800 $^{\circ}$C reveals that carbon increases from 0.087% at a hold time of 10 secs to a value of 0.102% at a hold

By increasing the amount of carbon in the martensite, there is less in the ferrite and since the ferrite is the dominant matrix phase, the ductility of the alloy is expected to increase. In addition, if the carbon is increased in the martensite, less carbon is available to form carbides. In order to examine the impact of various time at temperatures on carbide formation, the amount and size of carbides was determined from quantitative measurements. Figure 8 shows scanning electron microscope (SEM) images of samples isothermally held at 30 mins, 60 mins and 120 mins at 800 $^{\circ}$C. As the isothermal hold time increased, there was an increase in volume fraction of precipitates from 2.1 to 3.2%. However, the average size of the precipitates did not increase significantly with the various hold time indicating that the longer hold times, the precipitates were coarser and therefore less effective in strain-hardening the material. The accompanying SEM images show the larger precipitates in the sample isothermally held at two hours.
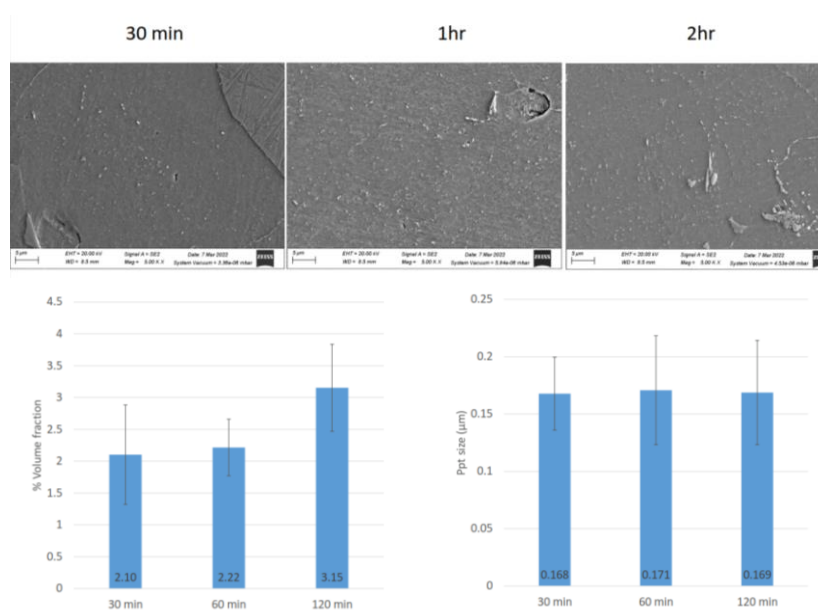

Figure 8: SEM photomicrographs of FSLA held for 30 mins, 1 hr. and 2 hrs. at 800 $^{\circ}$C showing frequency and size of carbides (top) and numerical values for volume fraction of carbides and size (bottom).

Based on all results of the metallographic analysis tensile properties were measured on the materials heat treated in the fashion described. Table III shows the tensile properties for the FSLA austenitized at 1200 $^{\circ}$C then furnace cooled to 800 $^{\circ}$C and held for 2 hours.

Table III: Tensile properties of FSLA Austenitized at 1200 $^{\circ}$C for 1 hr. then furnace cooled to 800 $^{\circ}$C for 2 hrs. then furnace cooled to room temperature.

Condition	UTS (MPa)	YS (MPa)	Elongation (%)	Hardness (HRA)
Ferrite Heat Treatment	604	326	23	49

4. Summary of Heat Treatments

It is apparent from the previous discussion that the FSLA alloy properties can be varied significantly by the manner in which it is heat treated after sintering. The alloys were initially developed as a replacement for a wrought DP600 which acquires its dual phase structure and mechanical properties through a combination of controlled rolling and intercritical anneal heat treatments. But in addition to the DP600 there are a number of DP alloys used in conventional wrought processing that have a range of ultimate tensile strengths varying from 480 MPa to 1050 MPa [9]. In many cases this is accomplished by increasing the carbon level to the same base chemistry. However, in the FSLA alloy, the wide range of microstructure (transformation products and ferrite) that can be achieved by

changing the intercritical annealing temperature along with the variation of the amount and size of the carbides, leads to a very flexible alloy in terms of mechanical properties. This is highlighted in Figure 9 where elongation versus ultimate tensile strength for both the wrought versions of dual-phase alloys (DP450, D490, DP590, DP780 and DP980) and the FSLA alloy are plotted. In the FSLA alloy, only the heat treatment is adjusted to tailor the mechanical properties so that development of print parameters is limited to one material and therefore saving a significant amount of development time.
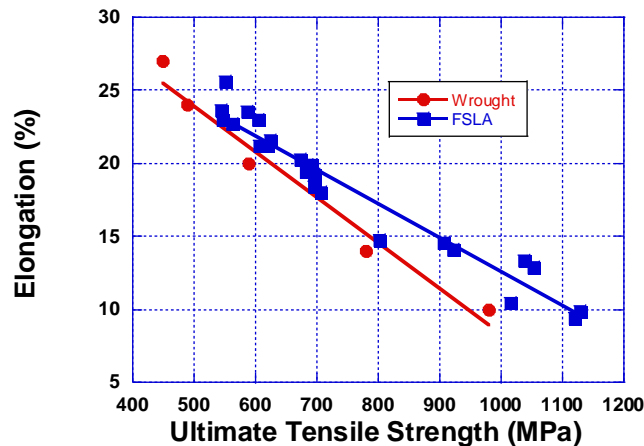

Figure 9: Mechanical properties of FSLA after different heat treatments. FSLA Alloy compared to conventional DP alloys with different Ultimate Tensile Strengths.

5. Summary and Conclusions

New technologies like MBJ require tailored materials to fully utilize their production potential. The FSLA material is designed and intensively tested for binder jetting. It is shown that FSLA presents good printability and sinterability. Of particular interest is the wide range of mechanical properties that can be achieved with one material without changing the printing and sintering process. The FSLA material properties can meet different requirements and can be tailored for different applications depending on the level of strength and ductility requires. Future work will focus on slight chemistry modifications to enhance the mechanical properties and their range beyond what was presented in this research.

Literature

[1]   World Steel Auto: http:\\www.worldautosteel.org
[2]   M.K. Singh, Application of Steel in Automotive Industry, Int. J. Emerging Technol. Adv. Eng. 6 (2016) 246–253.
[3]   C.C. Tasan, M. Diehl, D. Yan, M. Bechtold, F. Roters, L. Schemmann, C. Zheng, N. Peranio, D. Ponge, M. Koyama, K. Tsuzaki, D. Raabe, An Overview of Dual-Phase Steels: Advances in Microstructure-Oriented Processing and Micromechanically Guided Design, Annu. Rev. Mater. Res. 45 (2015) 391–431.
[4]   R.A. Kot and B.L. Bramfit, Editors, "Fundamentals of Dual Phase Steel," The Metallurgical Society of AIME, 1981.
[5]   C. Schade, T. Murphy, K. Horvay, A. Lawley and R. Doherty, Development of a Free Sintering Low Alloy (FSLA) Steel for the Binder jet Process, *Advances in Additive Manufacturing with Powder Metallurgy – 2021*, compiled by S. Atre and S. Jackson, Metal Powder Industries Federation, Princeton, NJ, 2021, part 7 pp.287-306 of Metals, Materials Research Forum LLC, 2018.
[6]   N.B. Shaw and R.W.K. Honeycombe, "Some Factors Influencing the Sintering Behaviour of Austenitic Stainless Steels," Powder Metallurgy, 1977; vol. 20: pp. 191-198.
[7]   R.I. Sands and J.F. Watkinson, "Sintered Stainless Steels I.- The influence of Alloy Composition upon Compacting and Sintering Behaviour," Powder Metallurgy, 1960, No. 5, pp.85-104.
[8]   DP600 Datasheet from Salzgitter Flachstahl, Edition 07/10, Page 1.
[9]   Voest Alpine Product Data Sheet for Dual Phase Steels, June 2019, page 3. https://www.voestalpine.com/stahl/en/content/